Posted on 26 Nov 2022 — The copyright holder is the author/funder. All rights reserved. No reuse without permission. — https://doi.org/10.1002/essoar.10510890.1 — This a preprint and has not been peer reviewed. Data may be preliminary.

Advanced classification of ionospheric troughs in midnight conditions

Alexander Karpachev[1]

[1]Pushkov Institute of Terrestrial Magnetism, Ionosphere and Radiowave Propagation, Moscow

November 26, 2022

Abstract

This study utilizes a novel technique to separate and classify different ionospheric troughs from CHAMP satellite data in the winter midnight ionosphere of the southern hemisphere at high solar activity (2000–2002). The main ionospheric trough (MIT) was separated from the high latitude trough (HLT). The separation was performed through an analysis of troughs in the frame of the model of the diffuse auroral particle precipitation. Two types of HLT were distinguished. In the mid-latitude ionosphere, the MIT was separated from the ring ionospheric trough (RIT), which is formed by the decay processes of the magnetospheric ring current. The separation was performed on the basis of an analysis of the prehistory of all geomagnetic disturbances for the period under study. In addition to the RIT, an equatorward decrease in the electron density, which is superimposed on the MIT and masks it, forms quite often at American and Atlantic longitudes.

Posted on 26 Nov 2022 — The copyright holder is the author/funder. All rights reserved. No reuse without permission. — https://doi.org/10.1002/essoar.10510890.1 — This a preprint and has not been peer reviewed. Data may be preliminary.

Supporting Information for

Advanced classification of ionospheric troughs in midnight conditions

Karpachev A.T.

Pushkov Institute of Terrestrial Magnetism, Ionosphere, and Radiowave Propagation (IZMIRAN), Kaluzhskoe Hwy 4, Troitsk, Moscow, 108840, Russia

The model of the auroral oval of precipitation

The model of auroral particle precipitation is based on data from a large set of DMSP satellites in the Northern and Southern hemispheres [Vorobjev and Yagodkina, 2005, 2010]. The model is uploaded on the website of the Polar Geophysical Institute: http://apm.pgia.ru. Figure S1 shows this model for quiet conditions AL = -10 nT, Dst = -5 nT (Kp~2). As can be seen from Fig.S1, the model describes three main zones of auroral particle precipitation**.**

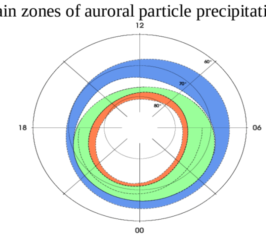

Figure S1. Model of auroral particle precipitation: diffuse auroral zone I equatorward of aurora (blue), structured auroral oval precipitation (auroral lights region or aurora, green), and soft diffuse precipitation zone II (orange) poleward of aurora.

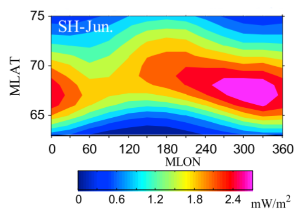

Figure S2. Longitudinal variations in the averaged auroral precipitation energy flux at 21 – 03 MLT under Kp = 2 for the June solstice (Jun.) in southern hemisphere [Luan et al., 2011]. Note, that plot is presented in geomagnetic longitude MLON.

1

Advanced classification of ionospheric troughs in midnight conditions

A.T. Karpachev

Pushkov Institute of Terrestrial Magnetism, Ionosphere, and Radiowave Propagation (IZMIRAN), 4, Kaluzhskoe Hwy, Troitsk, Moscow, 108840, Russia,

Corresponding author:
Alexander Karpachev, e-mail: karp@izmiran.ru

Key points:

- The high latitude trough (HLT), subauroral (main) trough (MIT), and mid-latitude ring trough (RIT) were classified from the CHAMP data.
- The HLT and MIT separation is based on diffuse auroral precipitation model with two zones, equatorward and poleward.
- The MIT and RIT were separated taking into account the prehistory of all geomagnetic disturbances for the period under study.

Abstract

This study utilizes a novel technique to separate and classify different ionospheric troughs from CHAMP satellite data in the winter midnight ionosphere of the southern hemisphere at high solar activity (2000–2002). The main ionospheric trough (MIT) was separated from the high latitude trough (HLT). The separation was performed through an analysis of troughs in the frame of the model of the diffuse auroral particle precipitation. Two types of HLT were distinguished. In the mid-latitude ionosphere, the MIT was separated from the ring ionospheric trough (RIT), which is formed by the decay processes of the magnetospheric ring current. The separation was performed on the basis of an analysis of the prehistory of all geomagnetic disturbances for the period under study. In addition to the RIT, an equatorward decrease in the electron density, which is superimposed on the MIT and masks it, forms quite often at American and Atlantic longitudes.

Plain Language Summary

There are several ionization troughs in the high and mid-latitude ionosphere. The regions of their existence overlap, thus presenting a problem in trough identification. The main issues are the separation of the high latitude trough (HLT) and the main ionospheric trough (MIT), as well as that of the MIT and the ring ionospheric trough (RIT). The problem of the HLT and MIT separation was solved by carefully analyzing the positions of the troughs relative to the equatorward boundary of the diffuse auroral precipitation model and the correspondence of the MIT polar wall to the equatorward diffuse precipitation zone and that of the HLT polar wall to the poleward precipitation zone. The subauroral MIT was also separated from the mid-latitude RIT, which is formed by the decay processes of the magnetospheric ring current and exists long in the recovery phase of even a weak geomagnetic disturbance. The separation of the MIT and RIT was performed on the basis of the analysis of the prehistory of all the geomagnetic disturbances for the period under study. In addition to the MIT, a decrease in the electron density, which is superimposed on the MIT minimum and masks it, occurs at America–Atlantic longitudes.

1 Introduction

The ionization trough was discovered from the Alouette I satellite data and was described by *Muldrew* (1965) as the main ionospheric trough (MIT). Since then, many studies have explored its characteristics, which have been described in reviews (*Ahmed et al.*, 1979; *Moffett and Quegan*, 1983; *Rodger et al.*, 1992; *Karpachev*, 2003). The greatest attention has been paid to the position of the MIT minimum (see, for example, (*Kohnlein and Raitt*, 1977; *Ahmed et al.*, 1979; *Oksman*, 1982; *Karpachev et al.*, 1996; *Werner and Prolss*, 1997; *Yang et al.*, 2015; *Deminov and Shubin*, 1918; *Aa et al.*, 2010; *Karpachev et al.*, 2022). These studies reported a large data scatter, which is due to the fact that the MIT can be confused with other troughs, including high latitude troughs (HLT) and low latitude troughs (LLT) (*Werner and Prolls*, 1988; *Karpachev and Afonin*, 1989, *Karpachev*, 2019). Thus, the problem of the separation and classification of ionospheric troughs arises. Significant progress in the separation of the MIT and HLT has been made in a previous study based on CHAMP data (*Karpachev*, 2019). The MIT is a subauroral structure because it is located equatorward of the auroral oval (*Rodger et al.*, 1992). The HLT is observed inside the auroral oval (*Grebowsky et al.*, 1983). With the simultaneous data on the precipitation of auroral particles, the separation of the MIT and HLT would be a routine task. However, particle precipitation on board the CHAMP has not been measured simultaneously; therefore, we were forced to use a statistical model of diffuse auroral precipitation. Thus, the current positions of troughs have been compared with some average positions of the equatorial boundary of the auroral oval (*Karpachev*, 2019). However, the current positions of the auroral oval and the troughs are often quite different from the average position. For example, the standard deviation for the MIT position is typically 2°–3°, and the data scatter is as high as ±10° (*Kohnlein and Raitt*, 1977; *Werner and Prolss*, 1997; *Aa et al.*, 2020). As a result, the highest latitude MIT case can be located inside the statistical auroral oval while the lowest latitude HLT case can be outside it.

In the present study, an advanced method is used. The key point is anthe application of a model of auroral precipitation obtained from the DMSP satellites data (*Vorobjev and Yagodkina*, 2005, 2010). This model describes the position of zone I diffuse precipitation at the equatorial edge of the auroral oval and zone II at its polar edge. As is known, the precipitation of zone I forms the polar wall of the MIT; meanwhile, the effects of zone II have never been considered. Moreover, the positions of both zones change with longitude (*Vorobjev and Yagodkina*, 2010; *Luan et al.*, 2011). Therefore, for superior efficiency, the analysis of the structures of the high latitude ionosphere was conducted herein on the basis of the framework of the longitudinal effect.

The problem of separating LLT from the subauroral MIT in the previous study was solved by removing from the CHAMP data set only the obvious cases of the so-called ring ionospheric trough (RIT) (*Karpachev*, 2019). The RIT is formed during the storm (substorm) recovery phase as a result of the decay of the magnetospheric ring current (*Karpachev*, 2021a, 2021b). However, equatorward of the MIT, in addition to the mid-latitude RIT, other electron density minima do not necessarily stand out as ionization troughs, but they significantly complicate the identification of the MIT. Therefore, this study also considered in detail the issue of the separation of the MIT and LLT.

Finally, to complete the pattern, this study highlighted the cases of a clearly expressed polar hole. In this way, the title of the paper can be interpreted broadly as the classification of electron density structures in the high and mid-latitude ionosphere. Within the framework of the advanced method, all the ionospheric troughs from the CHAMP data in the midnight winter ionosphere were thoroughly analyzed. As the main goal was to derive an accurate statement of the problem for trough separation, the analysis in the present study was limited to the southern hemisphere and high solar activity.

2 Observation data

The CHAMP satellite carried out *in situ* measurements of electron concentration *Ne* (Rother and Michaelis, 2019). Variations in *Ne* are presented below in terms of plasma frequency *fp* (Ne[cm^{-3}] = $1.24 \cdot 10^4 fp^2$[MHz]). The CHAMP altitude has changed from ~450 km to ~300 km, which is close to the height of the F2 layer maximum. It revolved on nearly polar orbit with the inclination of 87°. The CHAMP data time resolution of 15 s is less than 1° of latitude, which allows determining the minimum trough position accurately. The CHAMP data are available on the website http://op.gfz-potsdam.de/champ.

The CHAMP data for June, July, and August (i.e., for local winter conditions) in the southern hemisphere were used. The data only for high solar activity with F10.7 ~ 180 sfu for the period of 2000–2002 and the near-midnight conditions (23–01 LT) were considered. About 700 CHAMP passes in the winter high- and mid-latitude ionosphere for relatively quiet geomagnetic conditions with Kp < 4 were examined.

The MIT is usually defined by a fairly deep decrease in electron density of at least ~30%. We have not determined the level of electron density decrease in the MIT minimum. If the trough was poorly expressed on some satellite path or masked by ionospheric plasma irregularities, then the position of its minimum was determined through coordination with neighboring paths. Stricter criteria were imposed on the selection of the HLT. The HLT is observed in the auroral oval, where the electron density is highly irregular and a number of density minima can be observed. Therefore, the HLT was recorded only in the obvious cases wherein it was clearly structured and when its polar wall did not extend beyond the poleward diffuse precipitation zone. Similarly, the polar hole was defined only as a broad minimum of the electron density at latitudes above the poleward precipitation zone. Finally, only pronounced troughs were recorded equatorward of the MIT.

3 Structure of nighttime ionosphere

An analysis of the structures of the high latitude ionosphere was conducted using a model of auroral particle precipitation constructed from the DMSP satellites data in both hemispheres (*Vorobjev and Yagodkina*, 2005, 2010). The model is uploaded on the website of the Polar Geophysical Institute (http://apm.pgia.ru). In Figure S1 (in Supporting information), this model is presented for quiet conditions. The model describes three main auroral precipitation zones: diffuse auroral zone I equatorward of the auroral oval, structured auroral precipitation of the auroral oval (region of auroral lights, aurora), and zone II of the soft diffuse precipitation poleward of the aurora.

The boundaries of the precipitation zones in the near-midnight ionosphere change with longitude (*Vorobjev and Yagodkina*, 2010; *Luan et al.*, 2011), as well as the position of the MIT (*Karpachev et al.*, 2018). For the southern hemisphere, these boundaries are presented in Figure S2 (in Supporting information) according to (*Luan et al.*, 2011). The equatorward and poleward boundaries of the oval experience synchronous longitudinal variations with an amplitude of ~2.5°. Therefore, it is most effective to analyze the structures of the high latitude ionosphere in terms of geomagnetic latitude–geographic longitude. Figure 1 shows the positions of the different structures in the winter midnight (23–01 LT) ionosphere of the southern hemisphere. To eliminate the dependence on geomagnetic activity, the positions of the MIT, RIT, and HLT were reduced to Kp = 2 according to $\Lambda corr = \Lambda c - a(Kp(\tau) - 2)$, where Λc is the current position of the structure and the ***a*** factor is 2.0 for the MIT according to (*Karpachev et al.*, 1996), 1.5 for the RIT according to (*Karpachev*, 2021b), and ~1.5 for the HLT according to (*Grebowsky et al*., 1983). The Kp(τ) index was used as it considers the prehistory of geomagnetic activity development (*Deminov and Shubin*, 2018). In Figure 1, zones I and II of the diffuse precipitation taken from Figure S1 are shaded. The average (for all longitudes) position of the equatorial boundary of the auroral precipitation oval corresponds to 64° at Kp = 2 (*Karpachev*, 2019). The upper curve in Figure 1 corresponds to the CHAMP satellite inclination. The satellite inclination of 87° does not limit the observations of the discussed structures, except for the polar hole. But polar hole cases are shown in Figure 1 solely for the completeness of the pattern; only unambiguous cases were selected.

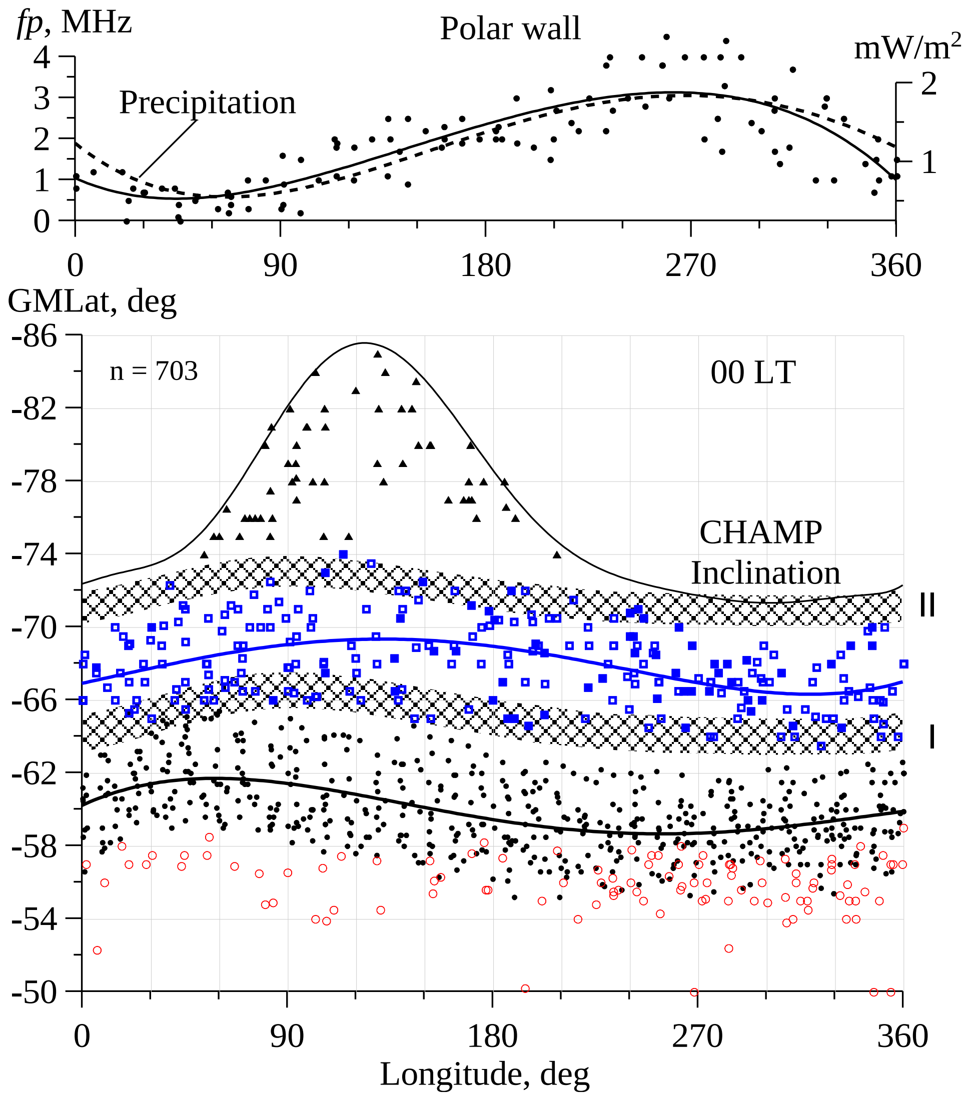

Figure 1. On the top: Longitudinal variations in the magnitude of MIT polar wall (dots and approximation) and averaged auroral precipitation energy flux at 21–03 MLT under Kp = 2 (dashed line) [*Luan et al.*, 2011]. On the bottom: Longitudinal variations in the positions of main structures in the near-midnight winter ionosphere of the southern hemisphere: polar hole (triangles), HLT1 (empty squares), HLT2 (filled squares), MIT (dots), RIT, and electron density minima (red circles). The shaded latitude belts show the diffuse auroral precipitation of zones I and II. The upper curve represents the CHAMP inclination equal to 87°.

The black dots in Figure 1 depict the cases of MIT observations (n = 703). The approximating curve demonstrates the longitudinal effect in the MIT position with an amplitude of ~3° and a correlation coefficient of 0.52. The scatter of the data (standard deviation) is 1.85°, which is less than the 2°–3° range that is usually observed in the statistical processing of trough data. In the first approximation, the variations in the MIT position are consistent with the variations in the position of the precipitation of zone I. The MIT was separated from the HLT (blue squares) at the high latitude boundary of the MIT occurrence region. Figure 2a shows the simplest case when both troughs are observed simultaneously. This case allows us to draw a fundamentally important conclusion: the MIT polar wall is, as usual, determined by the precipitation of zone I, and the HLT polar wall is undoubtedly formed by the precipitation of zone II. The latter fact is the key to the identification of the HLT type I. The HLT was previously studied in detail from *Ni* variations recorded on board OGO-6 at heights of 400–1,100 km (*Grebowsky et al.,* 1983) and from EISCAT radar data (*Williams et al.*, 1986). In particular, the statistical position of HLT relative to the auroral oval was determined (*Grebowsky et al.,* 1983). The authors observed the HLT exclusively within the auroral oval and attributed its formation ultimately to the action of electric fields in the zone of the high latitude ionospheric plasma convection. These fields cause the frictional heating of the plasma and its outflow upward; both cases lead to an increase in recombination and, consequently, to the formation of the trough. Since this effect is observed in a limited region, the HLT of this type is usually narrow (3°–5° in latitude). Such a trough is observed in Figure 2b together with the polar hole. We define such a trough as HLT2; it is depicted with crosses in Figure 1. Figure 2c shows a rather rare example of the simultaneous observation of the three troughs: MIT, HLT2, and HLT1. Figure 1 shows that HLT2 is observed less frequently than HLT1. In Figure 2, an approximation curve for all HLTs is drawn.

In the eastern hemisphere, at longitudes of 30°–90°E, the MIT is located at the highest latitudes so that the region of its existence overlaps with the precipitation of zone I and the region of HLT existence. In the region of the intersection of the two sets of troughs, the problem of separation becomes particularly acute. Therefore, all cases of trough observations in this region were analyzed thoroughly. The main result of this analysis was rather unexpected.

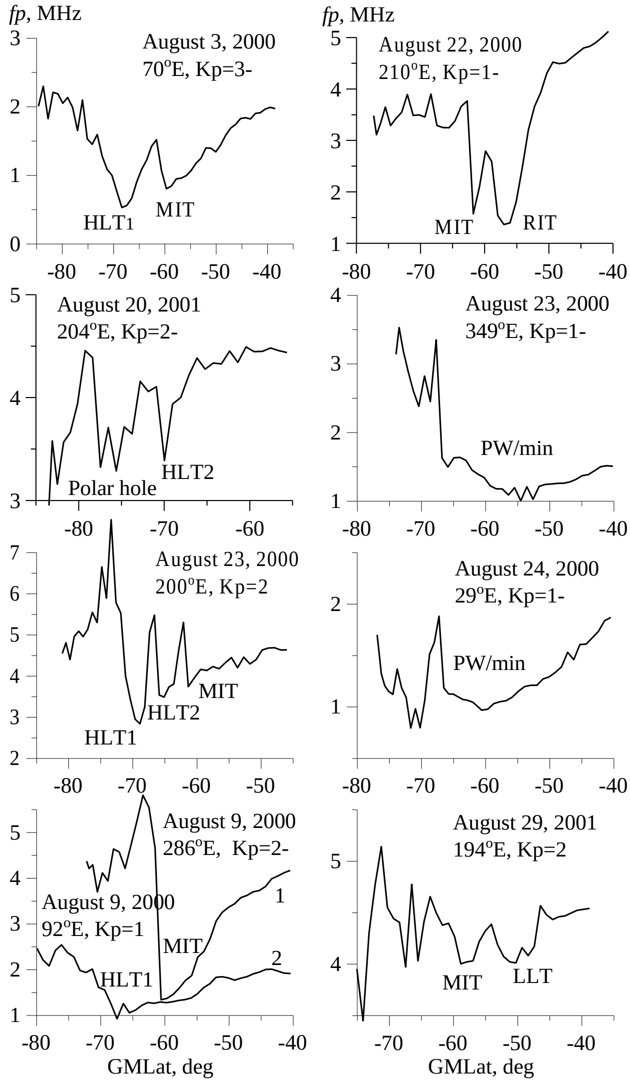

Figure 2. The most characteristic examples of troughs in the nighttime winter ionosphere of the southern hemisphere. Local time changes from 23.8 to 0.9 h. Details are in the text.

The top panel in Figure 1 shows the variations in the magnitude of the polar wall derived from the CHAMP data for the quiet period of August 15–24, 2000 (dots and approximation line). The dashed line depicts the longitudinal variations in the average electron flux calculated at latitude of −65° GMLat from the colored Figure 2S from (*Luan et al.*, 2011). As expected, the magnitude of the polar wall is completely determined by the precipitation. Electron precipitation is much stronger in the western hemisphere than in the eastern hemisphere. Therefore, in the western hemisphere, the precipitation forms a pronounced polar wall of the MIT, and it is always clearly determined. This illustrates the latitudinal *fp* cross-section 1 in Figure 2d, which represents the MIT recorded on August 9, 2000, at longitude of 286°E at 0.6 LT and Kp = 2-. Different scenarios can be realized in the eastern hemisphere. If the precipitation of zones I and II is still quite intense, they form (weak) peaks of electron density, and both troughs are observed. If the precipitation in one of the zones is very weak, then either the MIT or the HLT can be formed. For example, curve 2 in Figure 2d represents the latitudinal *fp* cross-section obtained on August 7, 2000, at longitude of 100°E at 0.5 LT and Kp = 1+. There is no peak of electron density; only the relative minimum of *Ne* at the MIT latitudes. Therefore, the MIT is not identified. The minimum of the electron density is observed much poleward at latitude of −68°, and it certainly belongs to HLT1 because its polar wall is formed by the precipitation of zone II. Note that this trough can be easily confused with the MIT in a cursory analysis. Finally, if both zones have no precipitation, then a monotonous decrease is recorded in the electron density to the pole without peaks and troughs. Such cases correspond to the value *fp* close to 0 in Figure 3.

The red circles in Figure 1 depict the troughs and quasi-troughs that were observed equatorward of the MIT. The main one among them is the RIT. It is formed during the recovery phase of a geomagnetic storm and even a weak substorm as a result of the decay of the magnetospheric ring current. The dynamics of this mid-latitude trough is described in detail in (*Karpachev*, 2021a, 2021b). When the MIT and RIT are simultaneously observed, their identification is not difficult; the equatorward trough is the RIT (Figure 2e). However, during a storm, any situation can be observed: both troughs, one MIT or one RIT. Moreover, the MIT can be identified on one path, and the RIT on the next path. Therefore, the main method of MIT and RIT separation is an analysis of the prehistory of the development of geomagnetic disturbance (*Karpachev*, 2021a, 2021b). Herein, even weak geomagnetic disturbances for the period under consideration were analyzed to separate the RIT from the MIT. An example of such an analysis is applied below in the discussion of Figure 3.

Figures 2f,g,h show examples of structures that can be defined as quasi-troughs. Figure 2f shows the latitudinal *fp* cross-section typical for the longitudes of America and the Atlantic. A steep polar wall of the trough, a shallow minimum of the electron density slightly equatorward (at −65.5°), and a deep and wide minimum at −55° are observed in Figure 2f. How is the position of the MIT determined in this case? The latitude of −65.5° for Kp = 1- corresponds rather to the polar wall of the MIT, and the latitude of −55° completely goes beyond the existence region of a “normal” MIT. Similarly, the position of the *Ne* minimum at latitude of −60.5° for Kp = 1- in Figure 2g is definitely lower than the “normal” position of the MIT at longitude of 29°E (Figure 1). The well-defined polar wall of the trough helps to solve this problem. In the near-midnight hours, the base of the polar wall usually coincides with the equatorial boundary of diffuse precipitation (*Rodger et al.,* 1986). The MIT minimum is located within 5° equatorward of this boundary (*Rodger et al.,* 1992), and the minimum distance is about 2° (*Slater et al*., 1980); therefore, the MIT minimum is usually 3°–4° equatorward of the polar wall. If the minimum of the MIT 3°–4° equatorward of the polar wall is determined in Figures 3f and 3g, then in both cases, the trough minimum will correspond to an average MIT position. As for the reason for the formation of an additional minimum of electron density, we should note that the geomagnetic latitude of −56° at longitude of 285° approximately corresponds to the geographical latitude of −66°, that is, the Arctic Circle. The Arctic Circle limits the area of the polar night in winter conditions, wherein there is no solar ionization and the electron density decays. The influence of the polar night affects a fairly wide range of longitudes from 120°W to 30°E.

Finally, Figure 2h shows an example of a clearly defined minimum of electron density recorded on August 29, 2001, at latitude of −50.2° and longitude 194°E. Several more well-expressed LLTs were observed at latitudes 50° and equatorward (not shown in Figure 1). They apparently belong to the class of LLTs discovered in (*Karpachev*, 2021c).

4 Events on August 19 and 21, 2000

Trough identification is obviously a challenge. In some cases, data analysis turns into a complicated investigation. Figure 3 shows two examples that required such an investigation. Figure 3 on the left shows the longitudinal variations of ionospheric structures for August 19 (top) and August 21 (bottom), 2000. The data were obtained in the near-midnight sector for the average value of Kp = 1 on August 19 and Kp = 2+ on August 21. However, at the beginning of August 21, the Kp index increased from a value of 1 to 3+, and this change was enough to form a deep RIT (red circles in Figure 3), which was then observed all day in a pronounced form. The examples are observed on paths 7, 15, and 25 in Figure 3 on the right. The MIT identification was a challenge. Its position was clearly defined only on paths 3 and 15. Conversely, the HLT was clearly revealed all day, as shown by the paths 3, 7, 15, and 25 on the right of Figure 3. In very quiet conditions on August 19, RIT did not manifest itself. On paths 2, 4, and 6, the MIT was clearly expressed, and its position could be determined either by the base of the polar wall (PW) or by the *fp* minimum (red circles), which formed clearly below the model position, as discussed previously. The rest of the time, the MIT manifested itself at best in the form of a small minimum of electron density, as observed on paths 14 and 24. HLT was also clearly manifested, particularly on paths 4, 14, and 24. On path 8, only HLT was observed. Therefore, in both cases, there was a well-expressed HLT, and on August 21, RIT was also well-expressed. Much effort was needed to distinguish the MIT in both cases. Moreover, on path 8 on August 19 under manual and automatic data processing, the HLT would have been identified as the MIT. Hence, we are skeptical about the automatic processing of data on the trough.

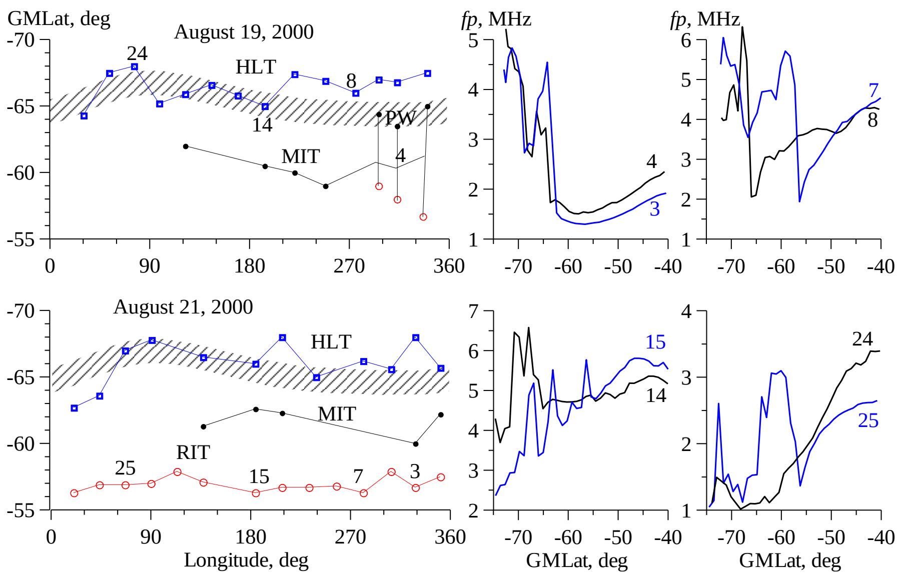

Figure 3. On the left: Longitudinal variations in the position of HLT (blue squares) and MIT (black circles) on August 19 (top) and August 21 (bottom), 2000. Red circles show the positions of the *fp* minima (top) and RIT (bottom). The shaded latitude belts show the diffuse auroral precipitation of zones I and II. On the right are the latitudinal profiles of *fp* for the paths marked in the Figure on the left.

5 Conclusion

Undoubtedly, considerable progress has been made in the separation and classification of the various structures of the nighttime high latitude and mid-latitude ionosphere. The success is based on several factors. First, the CHAMP large data set allows the consideration of a phenomenon from different angles. Second, all complex cases were analyzed carefully, and automatic data processing was found to be questionable. Third, the problem could only be solved after many years of experience. Note that the solution to the problem could be traced back to 1998 (*Karpachev*, 1998), and it was continued in 2019 (*Karpachev*, 2019). Fourth, the idea of separating MIT, HLT1, and HLT2 arose from a simple and illustrative model of diffuse auroral precipitation (*Vorobjev and Yagodkina*, 2005). It describes precipitation zone I on the equatorial edge of the auroral oval and zone II on its polar edge. It turned out that precipitation of zone 2 forms the PW of HLT1, similar to the way the precipitation of zone I forms the PW of the MIT. This point is key in the separation of MIT and HLT1.

As the boundaries of both zones change with longitude by 2.5° (*Luan et al.*, 2011), similar to the longitudinal variations in the MIT position, the analysis is most effective when performed in the framework of the longitudinal effect. The problem of the separation of MIT and HLT1 was found to be radically different in the western and eastern hemispheres. In the western hemisphere, the MIT is located at lower latitudes than in the eastern hemisphere and is equatorward of the auroral oval. In the western hemisphere, the intensive precipitation forms a very steep and high PW of the MIT. These conditions facilitate the separation of MIT and HLT. In the eastern hemisphere, MIT shifts to high latitudes so that the region of its existence at longitudes 30°–90°E overlaps with zone I of the precipitation and the region of HLT existence. In addition, the weak precipitation at longitudes of 0°–90°E produces much less expressed and irregular electron density structures. Therefore, at these longitudes, each case was considered especially carefully, and the separation of MIT and HLT1 was carried out according to the correspondence of the PW to the precipitation of zone I or II. The pattern is complicated by the presence of a second high latitude trough (HLT2) described in (*Grebowsky et al.,* 1983; *Williams et al*., 1986). Fortunately, HLT2 differs in that it is relatively narrow in latitude (3°–4°).

The mid-latitude troughs (and sub-troughs) located equatorward of the MIT were also clearly separated from the MIT for the first time. The main one among them is the RIT. It is formed even after a weak enhancement of geomagnetic activity, and it can be observed for a long time (sometimes for two days) at latitudes near L ~ 3 (*Karpachev*, 2021a, 2021b). It is no less difficult to separate the MIT from the RIT than the MIT from the HLT, but the methodology for such a separation has been carefully developed earlier (*Karpachev*, 2021a, 2021b). It is based mainly on the prehistory of the disturbance development. Therefore, even the weak geomagnetic disturbances during the period under consideration were carefully analyzed. Note that RITs are more often formed at longitudes with a weak geomagnetic field, i.e., in the western hemisphere.

The quasi-trough is understood as an additional minimum of the electron density equatorward of the MIT, and it is often observed at the longitudes of America and Atlantic. It is assumed to be related to the decay of the electron density beyond the polar circle during the polar night. This minimum deepens the MIT and therefore prevents the determination of the exact position of the MIT. Finally, several troughs too far from the mean MIT position (<50°) were recorded, and they, apparently, belong to LLTs (*Karpachev*, 2021c).

The result of this analysis is a more accurate determination of the MIT position: the standard deviation of 1.85° is less than that in other statistical studies, and the scatter has decreased to ±4°. This allows to significantly refine the model of the MIT position.

The study considers the structure of the ionosphere for limited conditions: high solar activity, winter, southern hemisphere, and near-midnight conditions. Preliminary analysis shows that the structure of evening and morning ionosphere is quite different from the considered structure. The same is particularly true for the daytime ionosphere. Consequently, this work should be considered as a statement of the problem, which implies the need for further research. The analysis of the structure of the evening and morning ionosphere is prepared for publication.

Acknowledgements. The author would like to thank sponsors and operators of the CHAMP mission; Deutsches GeoForschungsZentrum (GFZ) Potsdam and German Aerospace Center (DLR).

Open research. The CHAMP satellite carried out *in situ* measurements of electron concentration *Ne* (Rother and Michaelis, 2019). The CHAMP data are available on the website: https://dataservices.gfz-potsdam.de/panmetaworks/showshort.php?id=escidoc:4522906.

References

Aa, E., Zou, S., Erickson, P., Zhang, S-R., and Liu, S. (2020), Statistical analysis of the main ionospheric trough using Swarm in situ measurements, *J. Geophys. Res.*, *125*, e2019JA027583. doi.org/10.1029/2019JA027583.

Ahmed, M., Sagalyn, R.C., Wildman, P.J.L., and Burke, W.J. (1979), Topside ionospheric trough morphology: occurrence frequency and diurnal, seasonal and altitude variations. *J. Geophys. Res.*, *84*(2), 489–498. doi.org/10.1029/JA084iA02p00489.

Deminov, M.G., and Shubin, V.N. (2018), Empirical model of the location of the main ionospheric trough, *Geomagnetism and Aeronomy*, *36*(4), 45–52. doi.org/10.1134/S0016793218030064.

Grebowsky, J.M., Tailor, H.A., and Lindsay, J.M. (1983), Location and source of ionospheric high latitude troughs, *Planet. Space Sci.*, *31*(1), 99–105. doi.org/10.1016/0032-0633(83)90034-X.

Karpachev, A.T., Deminov, M.G., and Afonin, V.V. (1996), Model of the mid-latitude ionospheric trough on the base of Cosmos-900 and Intercosmos-19 satellites data. *Adv. Space Res.*, *18*(6). 221–230. doi.org/10.1016/0273-1177(95)00928-0.

Karpachev, A.T. (2003), Dependence of the MIT shape on longitude, altitude, season, local time, solar and magnetic activity, *Geomagnetism and Aeronomy*, *43*(2), 256–269.

Karpachev, A.T., Klimenko, M.V., and Klimenko, V.V. (2018), Longitudinal variations of the ionospheric trough position, *Adv. Space Res.*, doi.org/ 10.1016/j.asr.2018.09.038.

Karpachev, A.T. (2019), Variations in the winter troughs' position with local time, longitude, and solar activity in the Northern and Southern hemispheres. *J. Geophys. Res.*, *124*(10). 8039–8055. doi.org/10.1029/2019JA026631.

Karpachev, A.T. (2021a), Dynamics of main and ring ionospheric troughs at the recovery phase of storms/substorms. *J. Geophys. Res.*, *126*, e2020JA028079. doi.org/10.1029/2020JA028079.

Karpachev, A.T. (2021b), Statistical analysis of ring ionospheric trough characteristics. *J. Geophys. Res., 126*(10), e2021JA029613. doi:10.1029/2021JA029613.

Karpachev, A.T. (2021c). Sub-auroral, mid-latitude, and low-latitude troughs during severe geomagnetic storms. *Remote Sensing.*, *13*(3), 534; doi.org/10.3390/rs13030534.

Karpachev, A.T., Klimenko, M.V., Klimenko, V.V., Chirik, N.V., Zhbankov, G.A., and Pustovalova, L.V. (2022), Satellite model of foF2 in winter high-latitude ionosphere describing the trough structure. *Adv. Space Res.*, 69(1), 2-15. doi:10.1016/j.asr.2021.07.014.

Kohnlein, W., and Raitt, W.J. (1977), Position of the mid-latitude trough in the topside ionosphere as deduced from ESRO-4 observations. *Planet. Space Sci.*, *25*(5/6), 600–602. doi.org/10.1016/0032-0633(77)90069-1.

Luan, X., Wang, W., Burns, A., Solomon, S., Zhang, Y. Paxton, L. J. and Xu, J. (2011), Longitudinal variations of nighttime electron auroral precipitation in both the Northern and Southern hemispheres from the TIMED global ultraviolet imager. *J. Geophys. Res., 116,* A03302, doi:10.1029/2010JA016051.

Moffett, R.J., and Quegan S. (1983), The mid-latitude trough in the electron concentration of the ionospheric F-layer: A review of observations and modeling. *J. Atmos. Terr. Phys.*, *45*(5), 315–343. doi.org/10.1016/S0021-9169(83)80038-5.

Muldrew, D.B. (1965), F layer ionization troughs deduced from Alouette data. *J. Geophys. Res.*, *70*(11), 2635–2650. doi.org/10.1029/JZ070i011p02635.

Oksman, J. (1982). Apparent diurnal movements of the trough in total electron content (TEC) of the ionosphere. *Geophysica*, *19*(1), 13–22.

Rodger, A.S., Brace, L.H., Hoegy, W.R., and Winningham, J.D. (1986), The poleward edge of the mid-latitude trough – its formation, orientation and dynamics. *J. Atmos. Terr. Phys.*,*48*(8), 715–728. doi.org/10.1016/0021-9169(86)90021-8.

Rodger, A.S., Moffett, R.J. and Quegan, S. (1992), The role of ion drift in the formation of ionisation troughs in the mid-and high-latitude ionosphere – a review. *J. Atmos. Terr. Phys.*, *54*(1), 1–30. doi.org/10.1016/0021-9169(92)90082-V.

Rother, M., Michaelis, I. (2019). CH-ME-2-PLPT - CHAMP Electron Density and Temperature Time Series in Low Time Resolution (Level 2). GFZ Data Services.

Slater, D.W., Smith, L.L., and Kleckner, E.E. (1980), Correlated observations of the equatorward diffuse auroral boundary. *J. Geophys. Res.*, *85(2)*, 531–542. doi.org/10.1029/ja085ia02p00531.

Vorobjev, V.G. and Yagodkina, O.I. (2005), Effect of magnetic activity on the global distribution of auroral precipitation zones. *Geomagnetism and Aeronomy*, 45(4), 467–473.

Vorobjev, V.G., and Yagodkina, O.I. (2010), Seasonal and diurnal (UT) variation in the boundaries of the auroral precipitation and polar cup. *Geomagnetism and Aeronomy, 50*(5), 625–633. doi.org/10.1134/S0016793210050063.

Werner, S., and Prolss, G.W. (1997), The position of the ionospheric trough as a function of local time and magnetic activity. *Adv. Space Res., 20*(9), 1717–1722. doi.org/10.1016/S0273-1177(97)00578-4.

Williams, P.J.S., and Jain, A.R. (1986), Observations of the high latitude trough using EISCAT. *J. Atmos. Terr. Phys., 48*(5), 423–434. doi.org/10.1016/0021-9169(86)90119-4.

Yang, N., Le, H. and Liu, L. (2015), Statistical analysis of ionospheric mid-latitude trough over the Northern hemisphere derived from GPS total electron content data. *Earth, Planets and Space, 67*, 196. doi.org/10.1186/s40623-015-0365-1.